Fluorescent Probes

DOI: 10.1002/anie.201309691

Long-Wavelength Fluorescent Reporters for Monitoring Protein Kinase Activity**

*Nathan P. Oien, Luong T. Nguyen, Finith E. Jernigan, Melanie A. Priestman, and David S. Lawrence**

Abstract: *In vivo optical imaging must contend with the limitations imposed by the optical window of tissue (600–1000 nm). Although a wide array of fluorophores are available that are visualized in the red and near-IR region of the spectrum, with the exception of proteases, there are few long wavelength probes for enzymes. This situation poses a particular challenge for studying the intracellular biochemistry of erythrocytes, the high hemoglobin content of which optically obscures subcellular monitoring at wavelengths less than 600 nm. To address this, tunable fluorescent reporters for protein kinase activity were developed. The probing wavelength is preprogrammed by using readily available fluorophores, thereby enabling detection within the optical window of tissue, specifically in the far-red and near-IR region. These agents were used to monitor endogenous cAMP-dependent protein kinase activity in erythrocyte lysates and in intact erythrocytes when using a light-activatable reporter.*

In vivo optical imaging must contend with the limitations and opportunities imposed by the optical window of tissue (600–1000 nm).[1] Tissue transparency at wavelengths less than 600 nm is limited by the presence of hemoglobin and melanin whereas water is the chief culprit above 1000 nm. Fortunately, a wide array of fluorophores are available that are visualized in the red and near-IR[2] region of the spectrum and several of these have been covalently attached to antibodies for diagnostic purposes.[3,4] However, with the prominent exception of proteases,[5] there are few long wavelength probes for enzymes, a situation that is especially problematic with respect to intracellular erythrocyte biochemistry.[6] Unlike other mammalian cells, the high hemoglobin content of erythrocytes optically obscures subcellular monitoring at wavelengths less than 600 nm. To address the need for observing biochemical pathways in these cells, and with an eye on potential applications for tissue-based studies, red and far-red probes of protein kinase activity were designed.

[*] N. P. Oien, L. T. Nguyen, Dr. F. E. Jernigan, Prof. M. A. Priestman, Prof. D. S. Lawrence
Department of Chemistry, Division of Chemical Biology and Medicinal Chemistry, and the Department of Pharmacology
University of North Carolina, Chapel Hill, NC 27599 (USA)
E-mail: lawrencd@email.unc.edu

[**] We thank the National Institutes of Health for financial support (RO1 CA79954), Prof. Christian Doerig (Monash University) for bringing to our attention the role of PKA in erythrocyte function, and Prof. Karl Drexhage (ATTO-TEC GmbH; Universität Siegen).

Supporting information for this article (including experimental details) is available on the WWW under http://dx.doi.org/10.1002/anie.201309691.

Protein kinases catalyze phosphoryl transfer from ATP to hydroxy residues in proteins and peptides. Although a variety of fluorescent sensors for protein kinases have been described,[7,8] strategies have not yet been developed that can tune sensors to specific wavelengths within the optical window of tissue. One appealing approach is to take advantage of the commercial availability of far-red and near-IR fluorophores. Enzyme-catalyzed unquenching of fluorescence through the separation of a fluorophore from a nearby fluorescent quencher has been successfully applied to proteases.[5] Although we previously used such a strategy for protein kinases, the "unquenching" required the presence of a third party, namely stoichiometric amounts of a protein that sequesters the phosphorylated product.[9] We herein describe a much simpler and more robust alternative in which the newly introduced phosphate serves as a molecular trigger that drives the release of the fluorescent quencher. This provides access into the biologically useful far-red/near-IR wavelength realm as exemplified by visualization of kinase activity in the optically challenging intracellular domain of erythrocytes.

This strategy is outlined in Scheme 1. Our initial efforts focused on the cAMP-dependent protein kinase (PKA) because of its central role in erythrocyte behavior and the life cycle of the malarial parasite *Plasmodium Falciparum*.[10] PKA efficiently phosphorylates a diverse array of serine-containing positively charged sequences, and we employed two of these sequences in this study: Aoc-GRTGRRF*S*Y-amide[11] and KRRRLA*S*LAA-amide.[12] Fluorophores were

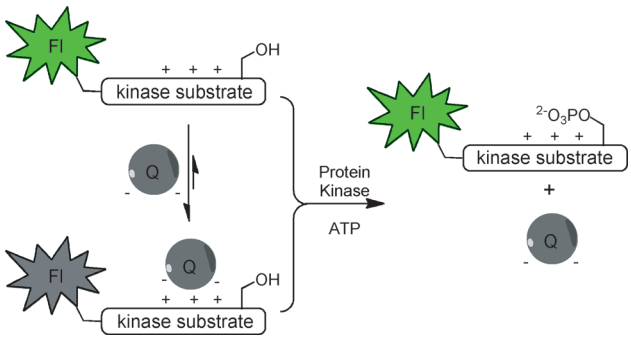

Scheme 1. General strategy for the protein kinase catalyzed unquenching of fluorescent kinase substrates. A positively charged fluorescent kinase substrate is quenched upon exposure to a negatively charged quencher dye (Q). Kinase-catalyzed phosphorylation releases Q as a result of favorable intramolecular electrostatic interactions between the newly introduced phosphate and positively charged substrate residues. Note: the nonfluorescent Q/kinase substrate complex in this study does not exist in a 1:1 stoichiometry.

appended to the N termini of both peptides. The amino octanoic acid (Aoc) moiety was used as a spacer in one of these to reduce any potential unfavorable steric clashes between the large fluorophores and the kinase active site. As noted below, this proved to be an unnecessary precaution because all of the peptides in this study serve as PKA substrates. A total of 14 fluorophores were examined that encompass a nearly 250 nm wavelength range throughout the red/far-red region ($\lambda_{ex} = 494$–727 nm, $\lambda_{em} = 530$–752 nm). For comparative purposes, the absorbances of five fluorophore-Aoc-GRTGRRFSY-amide peptides are shown relative to that of hemoglobin (Figure 1). We assessed the ability of

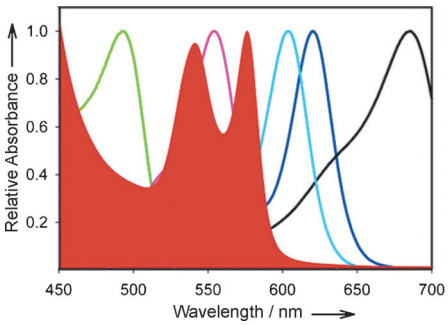

Figure 1. Relative wavelength-dependent absorbances of erythrocyte lysate (red) and fluorophore-Aoc-GRTGRRFSY-amide peptides where the fluorophore is 5Fam (green), TAMRA (violet), Atto620 (cyan), Atto633 (blue), or Red681 (black).

a library of 48 negatively charged dyes to quench the fluorescence of the fluorophore-substituted peptides (Table S5 in the Supporting Information). Upon subsequent addition of PKA and ATP, fluorescence recovery ranging from modest to dramatic was observed (Table 1 and Tables S6–S8 in the Supporting Information). We had previously shown that a phosphorylated residue in a PKA phosphopeptide product interacts with nearby arginine residues.[13] As a working hypothesis, we propose that this intramolecular electrostatic interaction displaces the quencher dye (Q) from the peptide, thereby resulting in the observed increase in fluorescence.

A few representative reporters are shown in Table 1. These agents respond to phosphorylation at wavelengths that span the green, red, far-red, and near-IR regions. Some of the most responsive fluorescence changes are observed when Acid Blue 80 (**1**; Scheme 2) is paired with either fluorophore-Aoc-GRTGRRFSY-amide or fluorophore-KRRRLASLAA-amide (Table S6). Although the fold changes observed with Evans Blue (**2**; Scheme 2) as the quencher are somewhat less dramatic, this dye appears to have a greater affinity for its peptidic counterparts than **1**. Since a Job plot analysis (Figure S10) revealed that the stoichiometry of the quencher/fluorophore–peptide pairs is not 1:1, we are unable to assign K_d values. Instead, we employed EQ_{50} as an assessment of affinity; that is, the [Q] that generates a fluorescence intensity halfway between [Q] = 0 and saturating Q. For example, in the case of TAMRA-Aoc-GRTGRRFSY-amide, the EQ_{50} values are (2.14 ± 0.05) μM for **1** and (0.15 ± 0.05) μM for **2** (Figures S11–S13).

Table 1: The PKA-catalyzed fluorescence increase (FI-fold) of the fluorophore-substituted peptides (2.5 μM) in in buffer [Tris-HCl pH 7.5 (25 mM), $MgCl_2$ (1 mM), where [**1**] is variable, see Table S6] and in 10% erythrocyte lysates [PBS buffer pH 7.4, $MgCl_2$ (5 mM), Halt protease and phosphatase inhibitor cocktail (1X), leupeptin (1 mM), **1** (150 μM)] with ATP (1 mM) and PKA (10 nM). Structures of the fluorophores are provided in Table S1.

Fluorophore–peptide	λ_{em}, λ_{ex} [nm]	Cond.	FI-fold↑
5Fam-Aoc-GRTGRRFSY	492, 518	Buffer	(2.5±0.1)
		Lysate	(1.3±0.1)
TAMRA-Aoc-GRTGRRFSY	550, 580	Buffer	(104±24)
		Lysate	(14.6±0.6)
Atto620-Aoc-GRTGRRFSY	619, 643	Buffer	(16.6±0.8)
		Lysate	(12.8±0.8)
Atto633-Aoc-GRTGRRFSY	635, 655	Buffer	(30.2±9.1)
		Lysate	(3.9±0.2)
Red681-Aoc-GRTGRRFSY	670, 706	Buffer	(11.2±0.6)
		Lysate	(3.4±0.1)

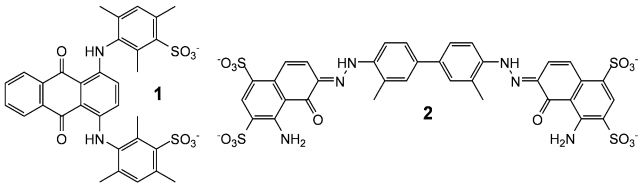

Scheme 2. Structures of quenchers **1** and **2**.

As validation of the presumed ability of these reporters to detect inhibitory activity, we employed fluorophore-Aoc-GRTGRRFSY-amide/**2** to examine the potency of two well-known inhibitors of PKA, H89 and KT5720. Both inhibitors block the phosphorylation of the Atto633-Aoc-GRTGRRFSY-amide substrate and, under the experimental conditions (1 mM ATP), they display IC_{50} values of (0.43 ± 0.15) and (0.61 ± 0.25) μM, respectively (Figure S14).

PKA plays key roles in erythrocyte senescence, localized vasodilation, and deformation.[14] Given the high hemoglobin concentration (≈ 5 mM) in erythrocytes,[15] clean observation of endogenous PKA activity should be more pronounced at wavelengths beyond 600 nm. We initially evaluated the ability of the fluorophore-Aoc-GRTGRRFSY-amide peptides to monitor endogenous PKA activity in 10% erythrocyte lysates. 5Fam-Aoc-GRTGRRFSY-amide displays very modest fluorescent enhancements upon phosphorylation in the presence of quenchers **1** (1.3-fold, Table 1) or **2** (1.04-fold, Table S10). By contrast, the fluorescence enhancement is significantly more robust with TAMRA-Aoc-GRTGRRFSY-amide (**1**: 14.6-fold; **2**: 7.3-fold) or Atto633-Aoc-GRTGRRFSY-amide (**1**: 3.9-fold; **2**: 6.3-fold).

Although the TAMRA-labelled peptide responds vigorously to phosphorylation in terms of absolute fluorescence fold change, the Atto633 species displays a superior signal to noise ratio (64:1 versus 12:1 for the TAMRA–peptide) for the progress curve (Figure 2). Indeed, whereas 90% of the

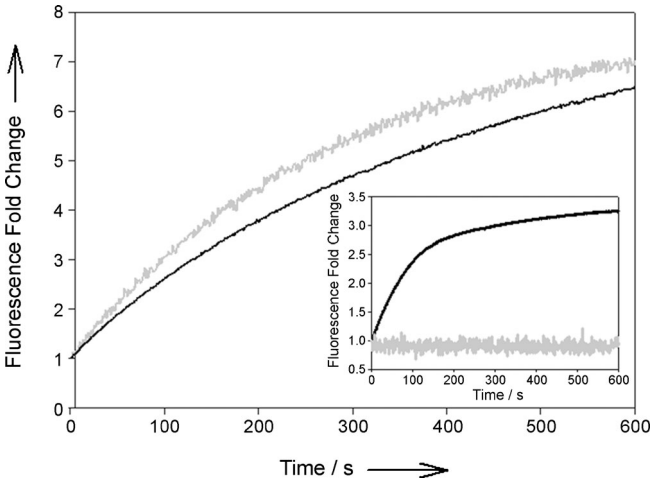

Figure 2. Reaction progress curve of the PKA-catalyzed phosphorylation of fluorophore-Aoc-GRTGRRFSY-amide (1 μM) with quencher **2** (2 μM) in 10% erythrocyte lysates where the fluorophore is Atto633 (black) or TAMRA (grey). Insert: in 100% lysate.

fluorescence signal is lost for the FAM–peptide and 98% for the TAMRA–peptide, only 10% of the signal is compromised in the case of the Atto633–peptide (Figure S17). Furthermore, the FAM and TAMRA fluorescence signals are completely obliterated in 100% erythrocyte lysates, whereas 50% of the original Atto633 signal is still present (Figure 2, insert). We also examined the effect of the dye quenchers **1** and **2** on erythrocyte viability and discovered that cellular integrity is markedly reduced upon exposure to **1** (30 μM), but remains unperturbed in the presence of **2** (30 μM; Figure S18). Consequently, all subsequent studies were performed with the Atto633-Aoc-GRTGRRFSY-amide (1 μM)/**2** (2 μM) sensor pair.

Since erythrocytes possess a number of protein kinases,[6] we investigated whether the observed fluorescence response displayed by Atto633-Aoc-GRTGRRFSY-amide/**2** is due to endogenous PKA activity. The moderately selective PKA inhibitor H89 blocks the observed fluorescence change with an IC_{50} of 1.14 ± 0.17 μM in 10% lysates (Figure S15 and Table S11). The highly selective PKA inhibitor KT5720 likewise prevents the phosphorylation-induced fluorescence response (IC_{50} 1.59 ± 0.36 μM). Finally, a PKA-specific antibody was employed to clear PKA from the lysates and phosphoryl transferase activity was then assessed. The 80% decrease in the phosphoryl transferase activity of the precleared lysate directly corresponds with the amount of PKA removed from the lysate (Figure S16). These results confirm that the fluorescence response in the lysate is driven by PKA activity.

There are a number of challenges associated with assessing intracellular enzymatic activity in cells, including controlling the start point ($t = 0$) of sensor phosphorylation. Light-activatable analogues provide a means to achieve this end.[16] The serine hydroxy moiety in Atto633-Aoc-GRTGRRFSY-amide was modified with a light sensitive 4,5-dimethoxy-2-nitrobenzyl (DNMB; Scheme 3) functional group to furnish probe **3**. As expected, both in buffer and in erythrocyte lysates, the modified serine residue in **3** is not phosphorylated

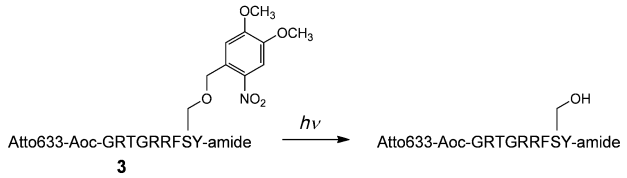

Scheme 3. Photolysis of probe **3**.

in the absence of photolysis. By contrast, upon illumination, the anticipated fluorescence increase is observed (Figure S19). In addition, the fluorescence response of the photochemically activated sensor is blocked in the presence of a PKA inhibitor.

Peptide **3** (1 μM) and quencher **2** (2 μM) were simultaneously introduced into erythrocytes under hypotonic conditions. Loading of the fluorescent peptide alone was confirmed by flow cytometry and confocal microscopy (Figures S20, S21). Erythrocytes loaded with peptide **3**/quencher **2** display a weakly fluorescent interior and a moderately fluorescent membrane (Figure 3). We suspect that during sensor loading, a portion of the positively charged peptide binds to and remains associated with the exterior of the cell membrane. The surface of erythrocytes is negatively charged as a result of proteins adorned with sialic acid.[17] Indeed, this property has been used to decorate red blood cells with a variety of positively charged nanoparticles.[18] The fluorescent ring that outlines the cell presumably reflects the

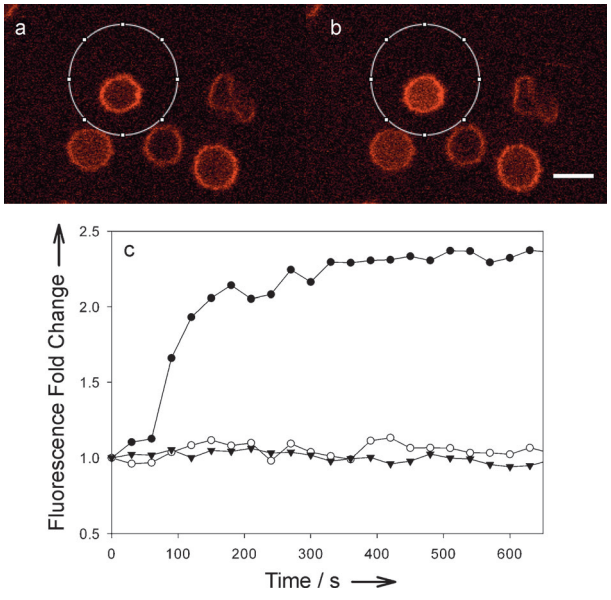

Figure 3. Confocal images of **2**/**3**-loaded erythrocytes a) before photolysis and b) 300 s after photolysis of the encircled cell. Photolysis was performed with a 50 mW, 405 nm laser (2% power level) in tornado mode with a dwell time of 20 μs/pixel and 25 frames. Imaging was performed with a 100X objective by using 635 nm at 4% laser power. Scale bar: 5 μm. c) Fluorescence fold change as a function of time where photolysis at 405 nm is applied at the third time point (filled circles), in the presence of KT5720 (triangles), and under depleted ATP (open circles). See Figure S22 for visual snapshots of the data plotted in part (c).

partial or complete displacement of the negatively charged quencher from the surface-bound fluorophore-labelled peptide.

PKA activity in intact erythrocytes was assessed by using confocal microscopy. Since UV illumination ($\approx$360 nm) is known to have an immediate untoward impact on hemoglobin biochemistry,[19] we employed a 405 nm laser to convert the DNMB–peptide **3** to its phosphorylatable counterpart. Upon photolysis, a rapid fluorescence response is observed in the interior of erythrocytes (Figure 3 and Figures S22–S25). By contrast, the membrane fluorescence remains unchanged as a function of time, a result that is expected if the fluorophore–peptide is simply appended on the exterior surface. In addition, the PKA-selective cell-permeable inhibitor KT5720 blocks the increase in Atto633 fluorescence otherwise observed in the erythrocyte interior. Finally, under conditions in which the intracellular content of the erythrocytes is depleted of ATP, no fluorescence response is observed. These results confirm that intracellular PKA phosphorylates Atto633-GRTGRRFSY-amide.

Electrostatic-driven recognition has served as a basis for the design of other sensors, such as those for heparin.[20] As one might expect, the number of opposing charges determines the apparent affinity of the quencher for the fluorophore–peptide.[9b] We have found that the electrostatic affinity of Aoc-GRTGRRFSY-amide/**2** is sufficient to construct a series of red and far-red sensors for protein kinase activity. The desired wavelength of visualization is easily "dialed-in" by appending the appropriate commercially available fluorophore. These reporters possess the requisite photophysical properties to take advantage of the most transparent optical region in tissue, as exemplified by visualization of protein kinase activity in erythrocytes.

Received: November 7, 2013
Revised: December 20, 2013
Published online: March 6, 2014

Keywords: biosensors · enzymes · fluorescent probes · peptides · signal transduction

[1] B. J. Tromberg, N. Shah, R. Lanning, A. Cerussi, J. Espinoza, T. Pham, L. Svaasand, J. Butler, *Neoplasia* **2000**, *2*, 26–40.
[2] L. D. Lavis, R. T. Raines, *ACS Chem. Biol.* **2008**, *3*, 142–155.
[3] S. Luo, E. Zhang, Y. Su, T. Cheng, C. Shi, *Biomaterials* **2011**, *32*, 7127–7138.
[4] Y. Nishimura, K. Yata, T. Nomoto, T. Ogiwara, K. Watanabe, T. Shintou, A. Tsuboyama, M. Okano, N. Umemoto, Z. Zhang, M. Kawabata, B. Zhang, J. Kuroyanagi, Y. Shimada, T. Miyazaki, T. Imamura, H. Tomimoto, T. Tanaka, *ACS Chem. Neurosci.* **2013**, *4*, 1183–1193.
[5] L. E. Edgington, M. Verdoes, M. Bogyo, *Curr. Opin. Chem. Biol.* **2011**, *15*, 798–805.
[6] A. D'Alessandro, P. G. Righetti, L. Zolla, *J. Proteome Res.* **2010**, *9*, 144–163.
[7] a) D. M. Rothman, M. D. Shults, B. Imperiali, *Trends Cell Biol.* **2005**, *15*, 502–510; b) M. C. Morris, *Biochim. Biophys. Acta Gen. Subj.* **2013**, *1834*, 1387–1395; c) Y. Li, W. Xie, G. Fang, *Anal. Bioanal. Chem.* **2008**, *390*, 2049–2057; d) D. Wu, J. E. Sylvester, L. L. Parker, G. Zhou, S. J. Kron, *Biopolymers* **2010**, *94*, 475–486; e) S. Martic, H.-B. Kraatz, *Chem. Sci.* **2013**, *4*, 42–59.
[8] N. V. T. Nhu, M. C. Morris, *Prog. Mol. Biol. Transl. Sci.* **2013**, *113*, 217–274.
[9] a) V. Sharma, R. S. Agnes, D. S. Lawrence, *J. Am. Chem. Soc.* **2007**, *129*, 2742–2743; b) R. S. Agnes, F. Jernigan, J. R. Shell, V. Sharma, D. S. Lawrence, *J. Am. Chem. Soc.* **2010**, *132*, 6075–6080.
[10] a) N. Wurtz, C. Chapus, J. Desplans, D. Parzy, *Parasitology* **2011**, *138*, 1–25; b) A. Merckx, G. Bouyer, S. L. Y. Thomas, G. Langsley, S. Egee, *Trends Parasitol.* **2009**, *25*, 139–144.
[11] D. B. Glass, H. C. Cheng, L. Mende-Mueller, J. Reed, D. A. Walsh, *J. Biol. Chem.* **1989**, *264*, 8802–8810.
[12] H. Flotow, G. Thomas, *J. Biol. Chem.* **1992**, *267*, 3074–3078.
[13] M. Prorok, D. K. Sukumaran, D. S. Lawrence, *J. Biol. Chem.* **1989**, *264*, 17727–17733.
[14] a) R. S. Sprague, M. L. Ellsworth, A. H. Stephenson, A. J. Lonigro, *Am. J. Physiol. Cell Physiol.* **2001**, *281*, C1158–C1164; b) H. K. Jindal, Z. Ai, P. Gascard, C. Horton, C. M. Cohen, *Blood* **1996**, *88*, 1479–1487; c) R. S. Sprague, E. A. Bowles, M. S. Hanson, E. A. DuFaux, M. Sridharan, S. Adderley, M. L. Ellsworth, A. H. Stephenson, *Microcirculation* **2008**, *15*, 461–471.
[15] S. E. Francis, D. J. Sullivan, D. E. Goldberg, *Annu. Rev. Microbiol.* **1997**, *51*, 97–123.
[16] a) C. Brieke, F. Rohrbach, A. Gottschalk, G. Mayer, A. Heckel, *Angew. Chem.* **2012**, *124*, 8572–8604; *Angew. Chem. Int. Ed.* **2012**, *51*, 8446–8476; b) P. Klán, T. Solomek, C. G. Bochet, A. Blanc, R. Givens, M. Rubina, V. Popik, A. Kostikov, J. Wirz, *Chem. Rev.* **2013**, *113*, 119–191; c) H. M. Lee, D. R. Larson, D. S. Lawrence, *ACS Chem. Biol.* **2009**, *4*, 409–427.
[17] E. H. Eylar, M. A. Madoff, O. V. Brody, J. L. Oncley, *J. Biol. Chem.* **1962**, *237*, 1992–2000.
[18] T. D. Mai, F. d'Orlye, C. Menager, A. Varenne, J.-M. Siaugue, *Chem. Commun.* **2013**, *49*, 5393–5395, and references therein.
[19] L. Pan, X. Wang, S. Yang, X. Wu, I. Lee, X. Zhang, R. A. Rupp, J. Xu, *PLOS One* **2012**, *7*, e44142.
[20] X. Fu, L. Chen, J. Li, M. Lin, H. You, W. Wang, *Biosens. Bioelectron.* **2012**, *34*, 227–231, and references therein.

